JOURNAL OF OPTOELECTRONICS AND ADVANCED MATERIALS, Vol. 11, No. 11, November 2009, p. 1723 - 1727

Multiple Quantum Well of GaAs VCSEL structure

FARAH Z. JASIM, KHALID OMAR*, Z. HASSAN
Nano-Optoelectronics Research and Technology Laboratory
School of Physics, Universiti Sains Malaysia
11800 Penang, Malaysia

The numerical investigation of the performance of 850 nm GaAs multiple quantum wells (MQW) vertical cavity surface emitting laser (VCSEL) structure was carried out. Laser technology-integrated program ISETCAD simulation has been used to enhance the device performance, we proposed a new model where a few low-doped distributed Bragg reflector (DBR) layers are introduced just after spacer layers in order to achieve a better matching of lattice constants, which finally provide high output power and better efficiency. Simulations have been performed for the analyses of several features of the VCSEL that primarily govern the operational characteristics of the device. All material parameters are evaluated based on the recent literature values.

(Received October 30, 2009; accepted November 12, 2009)

Keywords: Multiple Quantum Well, VCSEL, Doping concentration

1. Introduction

The various types of designs of vertical cavity surface emitting laser (VCSEL) and their specific applications have been reported [1, 2]. The VCSEL has been attracting great attention recently due to its general characteristics by single longitudinal mode operation, circular symmetric Gaussian beam profiles, high quality low divergence, low threshold current, wave-scale integration and simple packaging. The VCSEL offers the possibility of large 2-dimentional (2-D) array integration and low manufacturing cost of device [3-8]. Considering all these features, successful research on 850nm VCSELs could develop a standard technology to commercialize their applications in local area networks [9-14].Doping plays a critical role in increasing both the output power, radiative recombination and decreasing the threshold current.

Therefore doping can strongly affect the efficiency of the VCSEL laser through free carrier absorption loss [15-18]. In the present paper, the doping concentration effects on 850 nm (MQW) VCSEL are investigated using ISETCAD simulation program. We proposed a new kind of DBR formation for VCSELs which has much better matching of the lattice parameters. This is achieved by introducing a few low-doped layers just after the spacer layers within the different DBRs (this also helps to reduce the device series resistance). Simulation tools are used to determine the performance characteristics of the device in terms of the intensity distribution of the light output, output power, slope efficiency, material gain, refractive index dependence, etc. The proposed structure finally presents an excellent performance in the desired operating wavelength of 850 nm.

2. VCSEL design in numerical simulations

The ISETCAD program of laser simulation was used Finite element (FE) with vertical solver to solve the optical and electrical problems inside the VCSEL structure. A Fig. 1 shows the transverse cross-sectional view of the half portion of 850 nm GaAs/AlGaAs top surface emitting VCSEL with 2μ radius. In our design, the device has been constructed with n^+ - GaAs substrate followed by n^+-DBR. In order to get a good performance of the device, $Al_{0.20}Ga_{0.80}As$ (having high refractive index ~ 3.492) and $Al_{0.90}Ga_{0.10}As$ (having low refractive index ~ 3.062) materials were used for the p^- and n^+- type DBRs respectively.

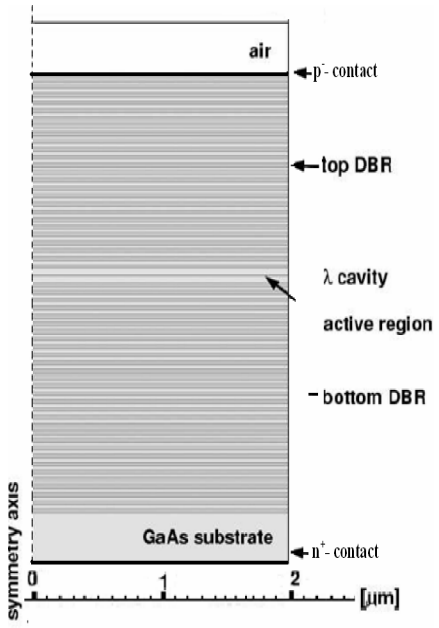

Fig. 1. A transverse cross-sectional view of the half portion of 850 nm GaAs/AlGaAs top surface emitting VCSEL

The lower section of the device contains thirty-eight pairs of n-DBRs with λ/4 thicknesses while the upper section of p-DBRs contains twenty pairs, less number of mirrors is taken in the p-type DBR section as compared to the n-type DBR to give finally less reflectivity in the upper section and enable the extraction of light from the p-type DBR with higher intensity, The active medium with λ-cavity length consists of four 6 nm GaAs quantum wells, separated by five $Al_{0.20}Ga_{0.80}As$ barrier with thickness of 12 nm. The multiple quantum well (MQW) was sandwiched by two spacers of $Al_{0.30}Ga_{0.70}As$.

3. Simulation results and discussion

To study the effect of doping concentration on the design, the doping concentration for both n and p-types DBRs was increased by 5 times in each step from $5 \times 1\ 0^{+17}$ cm^{-3} until $1 \times 1\ 0^{+20}$ cm^{-3} as shown in Fig. 2. We observed an increase in output power with increasing doping concentration of the DBR layers from 3.8 mW for $5 \times 10^{+17}$ cm^{-3} up to 137 mW for $1 \times 10^{+20}$ cm^{-3} doping concentration. This is attributed to the increasing the number of carriers (electrons and holes) in the active region which cause increase of radiative recombination inside the active medium and that leads to increase of output power.

Fig. 2 also shows the increased in the threshold current with increasing doping concentration of the DBR layers, which is due to the increasing on the diffraction losses between the carriers inside active medium.

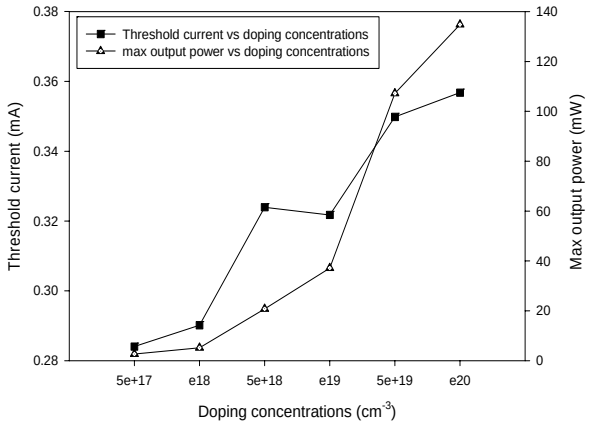

Fig. 2. VCSEL output power, and threshold current as a function of doping concentration.

The higher threshold current for our VCSEL indicated that more heat will be generated with time and thus decrease both the slope output efficiency and differential quantum efficiency (DQE) as shown in Fig. 3.

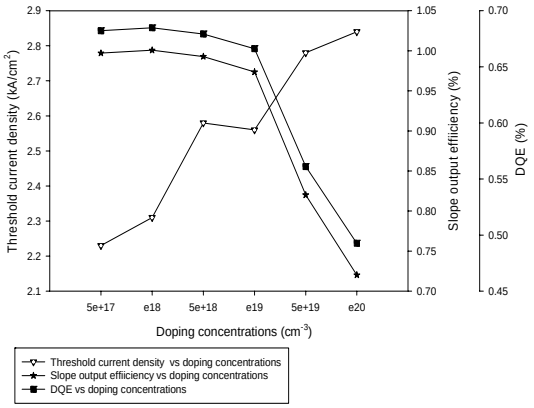

Fig. 3. VCSEL threshold current density, slope and differential quantum efficiency as a function of doping concentration.

In order to enhance the device performance and reduce diffraction losses inside the VCSEL cavity, we proposed a new model where three pairs of both p and n-type DBRs nearest to the active region, and which are in the proximity of the spacer are doped at $5 \times 10^{+17} cm^{-3}$ and the rest are doped highly at $1 \times 10^{+19} cm^{-3}$ concentration. In this case, proper matching of the lattice constants of the DBRs and the spacers can be achieved. This is essentially a very important aspect to be considered for the device fabrication. The device series resistance due to semiconductor heterojunction between all the material interfaces in the DBR can be reduced.

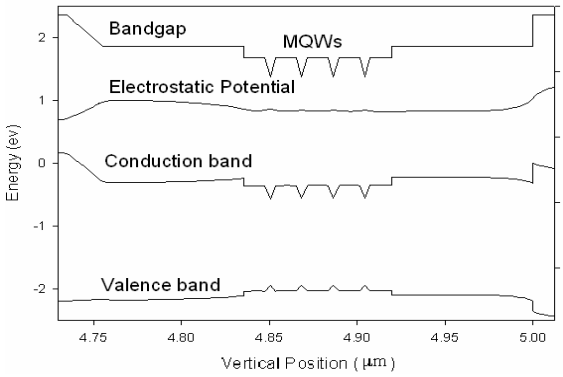

Fig. 4. Energy band diagram of MQW GaAs VCSEL

For the preliminary VCSEL structure under study, the energy band diagram and electrostatic potential of the MQW GaAs VCSEL are shown in Fig. 4.

The right side of the diagram is n-side and the left side is p-type of the VCSEL. The horizontal axis is the distance along the crystal growth direction (inside active medium). The optical material gain inside the quantum well and the carrier density are shown in Fig. 5 and Fig. 6 respectively. The quantum well in the left side (p-type) has higher optical material gain compared to the right side (n-type).

The electrons tend to be in the left quantum well.

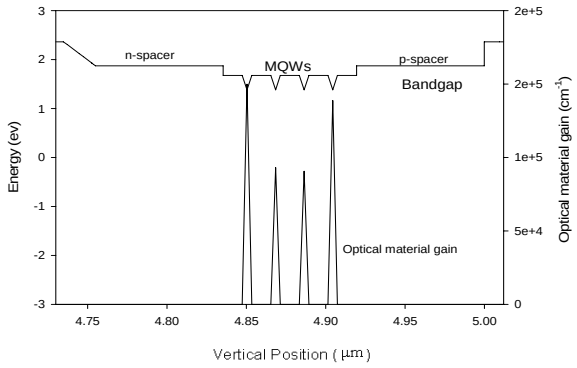

Fig. 5. Bandgap with optical material gain diagram of MQW GaAs VCSEL.

The holes have difficulty moving from left quantum well to right quantum well due to the relatively large effective mass, high band offset in the valance band, and low mobility so more holes are expected in the left quantum well. Since the left quantum well processes more electrons and holes as compared with the right quantum well, it has higher population inversion and hence higher stimulated recombination rate. Furthermore, the decay of the optical intensity is a little more in the bottom n-DBR section than the top p-DBR section. This is due to the higher number of DBRs present in the bottom part.

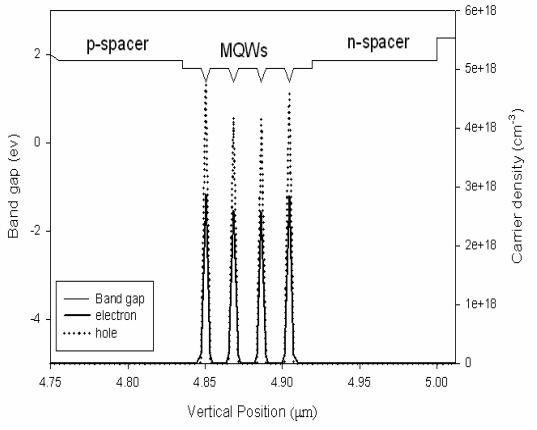

Fig. 6. Bandgap with carrier density diagram of MQW GaAs VCSEL

Fig. 7 shows the formation of the intensity together with refractive index in the VCSEL, which in turn, presents the intensity of the light generated within the MQW structure this indicates the presence of nodes and antinodes at the quarter-wavelength-thick DBR mirror interfaces. Also, it illustrates the existence of the MQW in the device, and we observe that the optical intensity is maximum within the MQW. We further notice that the decay of the optical intensity is a little more in the bottom n-DBR section than the top p-DBR section – this is owing to the higher number of DBRs present in the bottom part.

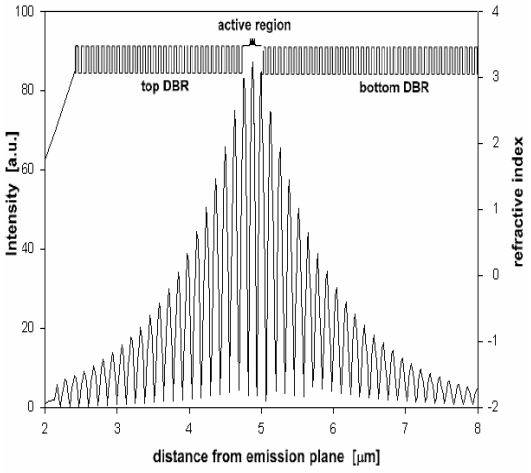

Fig. 7. The optical intensity together with the refractive index profile.

Fig. 8 shows the voltage and output power as a function of the injection current. An output power of 12.7 mW, threshold current of 280 μA, and the outer voltage of 2.5 V were obtained from cylindrical structure with radius 2 μm.The output slope efficiency and differential quantum efficiency (DQE) are the key performance parameters of the VCSEL. It was found that the slope efficiency of 0.999 and DQE up to 0.683 at an emission wavelength of 848.30 nm as shown in Fig. 9 and Fig. 10.

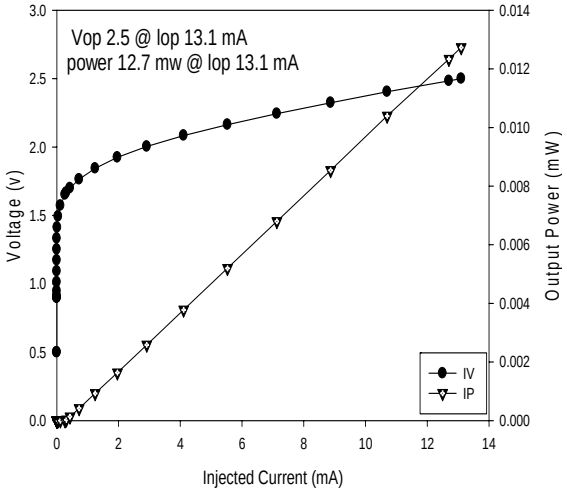

Fig. 8. Voltage and output power as a function of the injection current

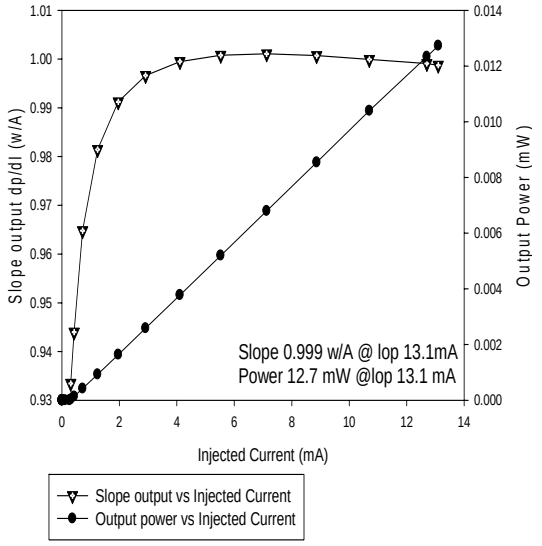

Fig. 9. Output slope efficiency, and output power as a function of the injection current.

In the case of 6 nm thick of the quantum well, the calculated resonant wavelength at 300 k is 848.3 nm, with peak mode gain 3680 (1/cm) as can be shown in Fig. 11**.**

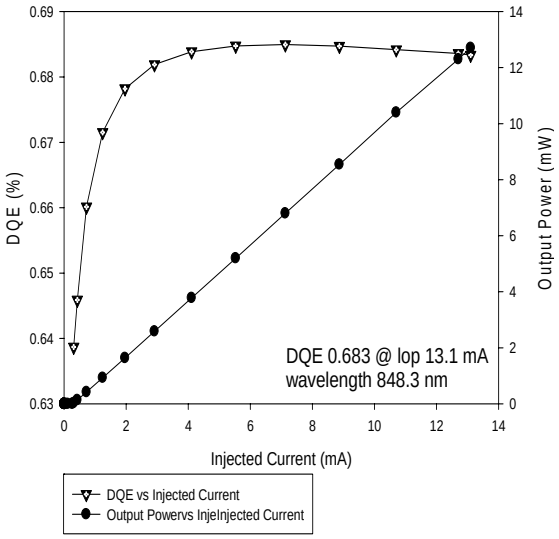

Fig.10. Wavelength and differential quantum efficiency as a function of the injection current

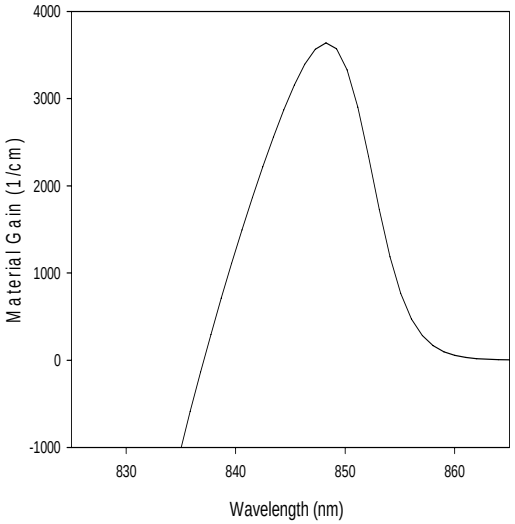

Fig.11. The mode gain of proposed MQWs VCSEL as a function of wavelength

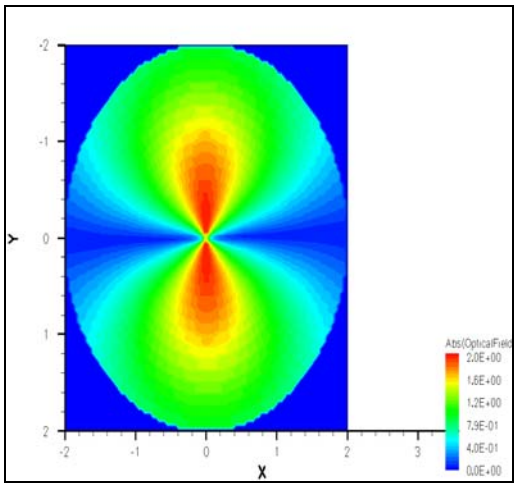

Fig.13. near field batten of proposed MQWs 850nm VCSEL laser design

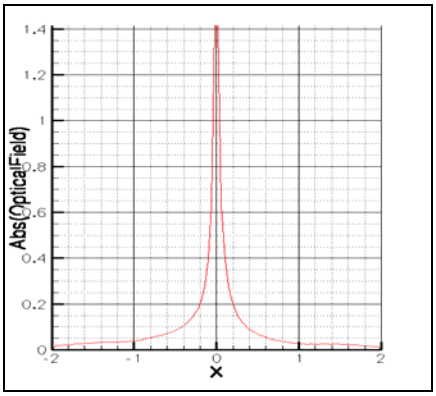

Fig. 14. The y-cut of the near field batten of proposed 850 nm MQWs VCSEL design.

Fig.13 and Fig.14 are shown the near field batten and y-axis of the near field respectively cut of proposed design with 850nm MQWs VCSEL design, which is shown the transverse mode, is actually a single order mode

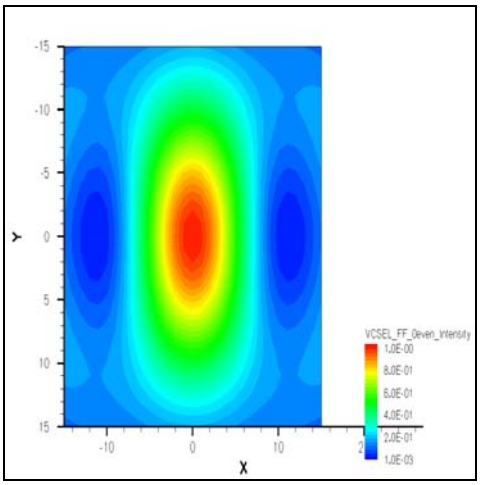

Fig. 15 The far field pattern of proposed MQWs VCSEL design.

The radiative pattern emanating from our proposed design are shown in Fig. 15 and Fig. 16 respectively, where $\theta_{//}$ and $\theta_{\perp}$ represent the full angle of half power in the directions parallel and perpendicular to the plan of the junction respectively the values of 12^{o} and 24^{o} are obtained for the FWHM $\theta_{\perp}$ and FWHM $\theta_{//}$, respectively. It was observed from the near field and far field that the transverse mode is actually a single order mode associated with the entire structure.

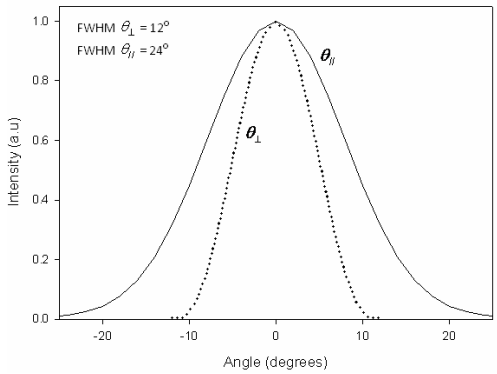

Fig.16 $\theta_{//}$ and $\theta_{\perp}$ far field pattern of proposed MQWs VCSEL design.

4. Conclusion

The effect of the doping concentration on output performance of GaAs MQWs VCSEL is numerically investigated. The influence of the DBR layers doping concentration on the output power, threshold current, slope and differential quantum efficiency is observed. In this study, a new kind of VCSEL with low-doped layers within the DBRs is proposed, which are introduced just after the spacer layers in order to achieve better matching of the lattice constants and minimize the device series resistance. As such, it is observed that this greatly improve the characteristic features of the device in terms of operation. It is noticed that the design of the proposed device resulted in excellent operational efficiency in the 850 nm of the electromagnetic spectrum. Details of the construction design of the VCSEL device are illustrated.

Acknowledgement

Financial support from Science Fund, MOST 1 and Universiti Sains Malaysia are gratefully acknowledged.

References

[1] S. M. Mitani, M. S. Alias, P. K. Choudhury, Proceedings of IEEE TENCON (TEN., 2006), pp. 264.
[2] C. W. Wilmsen, Vertical-cavity Surface-emitting Lasers: Design, Fabrication, Characterization, and Applications" (Cambridge University Press, Cambridge, 1999).
[3] F. H. Peters, M. H. MacDougal, IEEE Photon. Technol. Lett. **13,** 645 (2001).
[4] J. Piprek, P. Abraham, J.E. Bowers, IEEE J. Quantum Electron. **36,** 366 (2000).
[5] A. N. Al-Omari, K. L. Lear, Proc. SPIE **5364,** 73 (2004).
[6] M. Peeters, G. Verschaffelt, H. Thienpont, S. K. Mandre, I. Fischer, M. Grabherr, Opt. Express **13,** 9337 (2005).
[7] T. Gensty, K. Becker, I. Fischer, W. Elsaer, C. Degen, P. Debernardi, G.P. Bava, Phys. Rev. Lett. **94,** 233901 (2005).
[8] A. Tabaka, M. Peil, M. Sciamanna, I. Fischer, W. Elsaer, H. Thienpont, I. Veretennicoff, K. Panajotov, Phys. Rev. A **73,** 013810 (2006).
[9] H. J. Unold, S. W. Z. Mahmoud, Proc. SPIE **3946,** 207 (2000).
[10] P. Damberg, L. Erdmann, R. Bierbaum, A. Krehl, A. Brau¨er, E. B. Kley, Microsyst. Technol. **6,** 41 (1999).
[11] J. Piprek, A. Black, P. Abraham, E. L. Hu, J. E. Bowers, Proceedings of CLEO, (1999), paper CTh06.

*Corresponding author: frlaser@yahoo. com,